Ignition Performance and Reaction Dynamics of DMAZ/DN-10 Composite Fuel and N_2O_4 Oxidant: DFT-based calculations and experimental verification

Minna GAO *, Xiaomeng LV *, Ying JIA, Guofeng JIN, Jun SU, Keke SHEN

Rocket Force Engineering University, No. 2 Tongxin Road, Baqiao District, Xi'an City, Shaanxi Province, 710025, China

http://doi.org/10.5755/j02.ms.42650

Received 4 September 2025; accepted 26 November 2025

DMAZ (2-dimethylaminoethylazide) is a liquid rocket fuel, which is considered a lucrative spacecraft propellant to replace the toxic monomethylhydrazine, while DN-10 (1,10-diazidodecane) is a new type of synthesized high-energy fuel with 1,10 positions of the alkyl group substituted by azide, making it higher energy. This study investigated the DMAZ/DN-10 formulated fuel performance experimentally and theoretically via the density functional theory (DFT), revealing increased density and significantly enhanced combustion heat compared with pure DMAZ. However, its ignition required heating. The ignition delay, active sites, reactivity, and hydrogen abstraction barrier were determined based on DFT calculations. The DN-10 reactivity was lower than that of DMAZ, and the transition-state barrier of DN-10 in hydrogen abstraction was higher than that of DMAZ, implying that hydrogen abstraction of DN-10 required more energy and exhibited a larger enthalpy change than DMAZ. Therefore, DN-10 ignition did not occur at room temperature but succeeded at elevated temperatures. This study results are considered instrumental in the substantiated optimization of formulated fuels.

Keywords: DMAZ, DN-10, combustion heat, ignition delay, density functional theory.

1. INTRODUCTION

Hydrazine fuel is commonly used in aerospace and military fields as the core fuel for the self-igniting liquid propellant [1, 2]. However, hydrazine fuel has high volatility, high toxicity, strong carcinogenicity, etc., with severe environmental pollution and health hazards. In particular, and it can poison the refuelling personnel through the respiratory tract, skin, wounds, digestive tract, etc. Hence, the research and development of a new type of more environmental-friendly propellant with high density, low freezing point, high energy ratio, and low pollution risks is an urgent problem to be solved by the liquid propellant industry [3, 4].

2-dimethylaminoethylazide or 2-azido-N,N-dimethylethanamine (DMAZ) is an amine organic substance substituted by a high-energy group [5, 6]. It has been demonstrated that the density of DMAZ is large, the freezing point is low, the combustion product is clean, the specific impulse is high, the combustion speed is high, and it is almost non-toxic, not carcinogenic, etc. Introducing the azide group leads to increased nitrogen content and decreased hydrocarbon content, which can effectively reduce the fuel's flame temperature and temperature signal, so it is considered the ideal fuel to replace the hydrazine fuel applied to liquid propellant. Although DMAZ has good overall performance, compared with hydrazine propellant, its combustion heat must be further improved, and the ignition delay must be shortened [7 – 11].

Another innovative synthesized high-energy fuel is 1, 10-diazidodecane (DN-10), which 1,10 positions of the alkyl group are substituted by azide. Therefore, DN-10 is a promising green high-energy fuel due to its higher density and energy than the azide alkane. Based on the previous research conducted by the research group on optimizing the performance of DMAZ by adding decane, this paper introduces higher energy decane DN-10 substituted with azide groups into DMAZ to form a higher energy composite fuel DMAZ/DN-10, and analyzes its improvement on the overall performance of DMAZ. However, few studies on DN-10 have been reported, and its characteristics require more research.

Since experimental studies fail to clarify reaction mechanisms, it is necessary to carry out theoretical microanalysis to improve the combustion heat and shorten the ignition delay. Density functional theory (DFT) can simulate molecular reactions and demonstrate the reaction process, which can help researchers analyze the reaction mechanism from the molecule-level perspective and then optimize the formulation [12 – 15]. Considering the practical value and speed advantage of the B3LYP hybrid functional in geometry optimization, the B3LYP hybrid functional was selected for structural analysis in this study to ensure high accuracy, efficiency, and wide applicability to molecular systems. B3LYP (Becke, 3-parameter, Lee-Yang-Parr) is a widely used hybrid density functional, which introduces the Hartree-Fock (HF) exact exchange energy based on the traditional DFT, which significantly improves the accuracy of the calculation, and is especially suitable for the calculation of organic molecules, reaction barriers, and thermodynamic properties. Zhang et al. [16] explored reactions of DMAZ with HNO_3 and NO_2 by using B3LYP DFT, and identified two low-temperature reaction pathways. Türker et al. [17] investigated static images of the interactions between the components in the absence of any spontaneous combustion reaction and found that under vacuum conditions, DMAZ and TEMED are mainly electrostatic to maintain their electronic integrity; spontaneous combustion may be triggered if suitable

* Corresponding author: M. Gao
E-mail: *314578743@qq.com*

physical, chemical, or catalytic conditions are present. Wu et al. [1] reported that DMAZ decomposes at temperatures as low as 600 K, increasing chamber pressure. DMAZ decomposes mainly through the breakage of N-N_2 bonds, the main reaction pathway in its spontaneous combustion process. Chen et al. [18] performed DFT calculations on the thermal decomposition of DMAZ and found that the main pathway is the reaction between the breakage of N-N_2 bonds and the formation of mono- or triplet-nitroso groups.

2. EXPERIMENTAL AND THEORETICAL METHODS

At B3LYP/6-31G+(d, p) level of theory, the geometrical conformations of DMA, DN-10, and N_2O_4 are optimized to generate the files with wave function information, and the most stable conformations of various substances are found based on the wave function analyses, and then, based on the wave function analyses. Then, the reactivity of each substance is determined by calculating the energy difference between LUMO and HOMO, and the most probable active sites are found by Fukui function calculation, and the active sites are determined by comparing with the average localized ionization energy (ALLE) results [19 – 20]. The geometries of reactants, products, and intermediates in the DMAZ, DN-10, and N_2O_4 reaction pathways are optimized at the B3LYP/6-31+G (d, p) level of theory. The frequencies of the optimized conformations are analyzed to confirm that the frequencies of the resulting reactants, products and intermediates are all positive, and single-point energy calculations are carried out; the geometrical conformation of the transition states in the reaction paths of DMAZ, DN-10, and N_2O_4 is searched by using the traditional transition state theory (TST). By analyzing the frequencies of the searched conformations, it can be confirmed that the frequencies of the obtained transition states are positive, except for one, which was null.

A calibrated graduated pipette was used to pipette DMAZ into the sample vial quantitatively, and a certain amount of DN-10 solution was pipetted with a micropipette to formulate 20 mL of DMAZ/DN-10 formulated solution with 10 %, 30 %, 50 %, and 70 % DN-10 (volume fraction), as shown in Table 1.

Table 1. DMAZ/DN-10 formulated fuel with different mix ratios (volume fractions)

Volume fraction of DN-10, %	Volume of DN-10, mL	Volume of DMAZ, mL
0	0	20
10	2	18
30	6	14
50	10	10
70	14	6
100	20	0

3. RESULTS AND DISCUSSION

3.1. Performance characterization

3.1.1. Miscibility

The transmittance of the formulated fuel measured by the haze meter is shown in Fig. 1. As indicated, the overall transmittance of formulated fuel samples with different contents of DN-10 was good, and the average transmittance remained above 89.40 % after 30 days of resting, indicating that DMAZ and DN-10 are miscible. With the increase of the content of DN-10, the transmittance of the formulated fuel showed an increasing trend, indicating that DN-10 fuel is more pure and transparent.

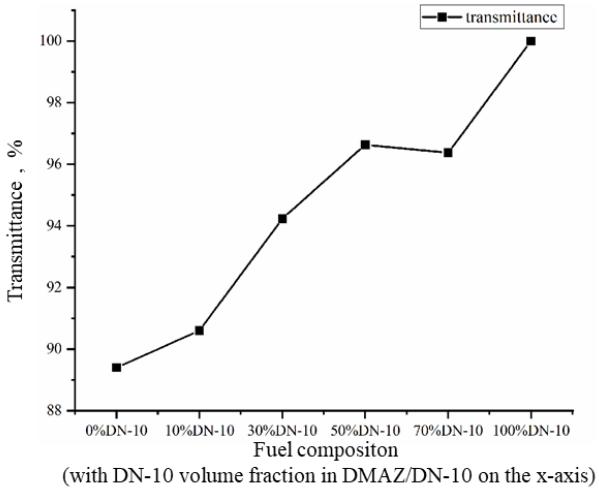


Fig. 1. Transmittance of formulated fuel samples with different contents of DN-10

3.1.2. Density

The densities of the formulated fuel samples with different DN-10 contents were determined using the DSY-412 petroleum density tester. As shown in Table 2, the densities of all the formulated fuel samples were increased compared with DMAZ, and the densities were proportional to the DN-10 content. For example, the density of the formulated solution with 70 % DN-10 is 0.964 g/cm³, which is 3.1 % higher than that of DMAZ. It can provide more energy to the aircraft when the volume of the fuel storage tank remains unchanged, which can satisfy the requirement of high-density fuels for future aircraft development.

Table 2. Density of different formulated fuel samples

DN-10 content, %	Density, g/cm^3
0	0.935
10	0.939
30	0.947
50	0.958
70	0.964
100	0.975

3.1.3. Viscosity

The viscosity of formulated solutions with different contents of DN-10 at -50 ℃, -40 ℃, -20 ℃, 0℃, and 20 ℃ was determined by using a low-temperature motion viscosity tester. As shown in Fig. 2, the viscosity of all formulated fuel samples increased as the temperature decreased. Formulated fuel samples with 50 % DN-10 or above showed solidification at -50 ℃, while formulated fuel with 30 % DN-10 or less showed low-temperature viscosity comparable to DMAZ. At a fixed temperature, the viscosity of formulated fuel increased with the content of DN-10, indicating that the viscosity of DN-10 was larger than that of DMAZ. Hence, it is recommended that the content of DN-10 in formulated fuel is below 30 %.

3.2. Combustion heat

Weighing 0.508 g of the fuel solution, an oxygen bomb calorimeter was used to test the total and net combustion heat of different ratios of formulated fuel. According to Fig. 3, the low-level combustion heat (net combustion heat) of DMAZ was 6123 Cal/g, the low-level combustion heat (net combustion heat) of DN-10 was 7122 Cal/g, significantly higher than DMAZ, under the same conditions, DMAZ exhibits better combustion performance. With the content of DN-10 gradually increasing, the high-level combustion heat (total combustion heat) and net combustion heat of the formulated fuel gradually increased, consistent with the analysis results. the net combustion heat of formulated fuel with 10 % DN-10 increased by 4.5 %, and the net combustion heat of formulated fuel with 70 % DN-10 increased by 12.1 %. Hence, the addition of DN-10 can significantly increase the net combustion heat of formulated fuel, which can provide more energy to aircraft under the same conditions and meet the development demands in the future.

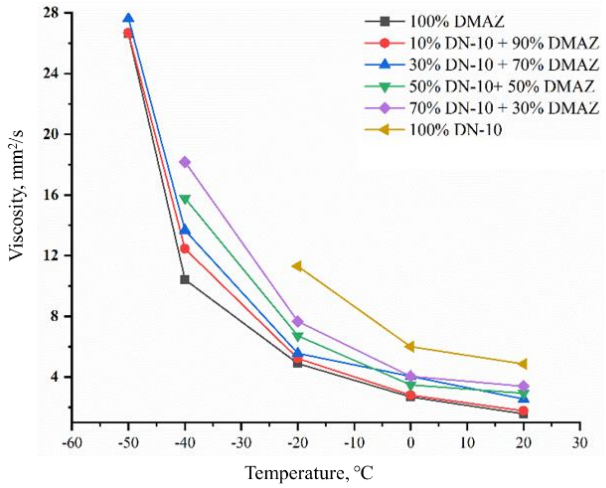


Fig. 2. Viscosity of different formulated fuels at different temperatures

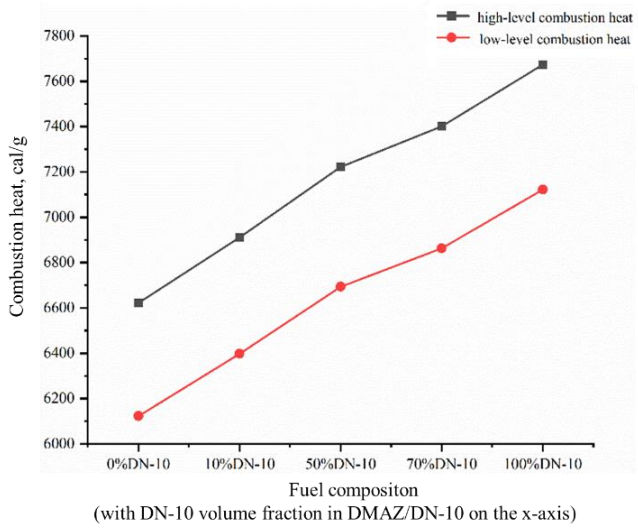


Fig. 3. High- and low-level combustion heat values for DMAZ/DN-10 formulated fuels

3.3. Ignition delay stage

The DN-10/DMAZ formulated fuel ignition delay was measured using a self-constructed high-speed camera-based experimental setup. A 100 μL microsyringe was used to control the fuel drops, and one drop of formulated fuel (~10 μL) was dropped at a time at a uniform height of 5 cm above the beaker. The beaker (25 mL) was placed directly under the microsyringe, and about 4 mL of N_2O_4 was removed and placed in the beaker. Using a high-speed camera to capture photos of the process from fuel depletion to contact with oxidants until ignition. The delay period of the ignition t_{id} is derived as follows:

$$t_{id} = t_2 - t_1 \quad (1)$$

where t_1 is the time of the initial fuel contact with the oxidant level; t_2 is the moment of apparent fire occurrence.

The results showed that DMAZ ignited spontaneously at room temperature (RT) in contact with N_2O_4 (ignition delay ≈ 194 ms), with none of the formulated fuel samples igniting spontaneously at room temperature. When the formulated fuel with 10 % DN-10 was heated up to 35 °C, it ignited in contact with N_2O_4, and the ignition delay stage was 111 ms. In other words, DN-10 requires higher energy to ignite than DMAZ. To analyze the reason for this, DFT was used to analyze the microscopic reaction.

3.4. Reaction kinetics of DMAZ/DN-10 formulated fuel with N_2O_4

3.4.1. Structural optimization

Before carrying out the reaction kinetics study, it is necessary to determine each substance's most stable structure; the lower the energy, the more stable the molecular structure. Firstly, based on the molecular structures of DMAZ, DN-10, and N_2O_4, we set up typical initial configurations, and after optimization by Gaussian software, we find a stable configuration by calculating and comparing the energies of different configurations. According to Fig. 4 – Fig. 6, a – for the assumed possible initial configuration; b – is the optimized optimal configuration.

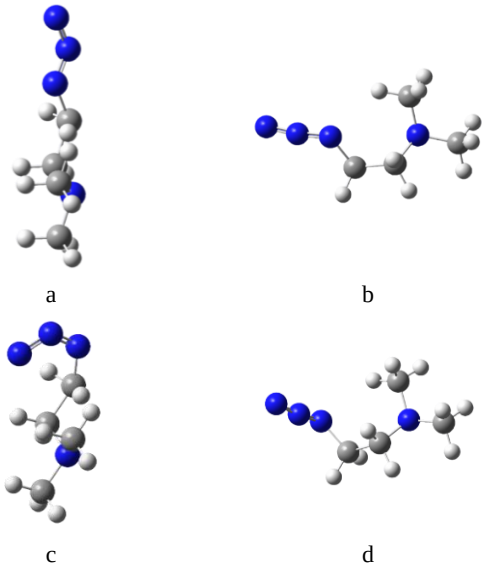


Fig. 4. DMAZ configurations: a – I initial; b – I optimized; c – II initial; d – II optimized

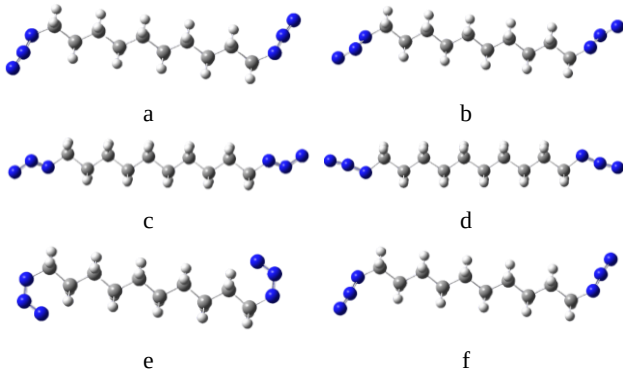


Fig. 5. Configurations of DN-10: a – I initial; b – I optimized, c – II initial; d – II optimized; e – I initial; f – II optimized



Fig. 6. Configurations of N_2O_4: a – initial; b – optimized

DMAZ assumed two different initial configurations, and after optimization, it was found that the energies of the two different initial configurations are as follows: the energy of the left configuration is -377.228 Hartree, the energy of the right configuration is -377.228 Hartree, and the energy is the same, therefore, the optimized configuration is the stable configuration of DMAZ. DN-10 sets three typical initial configurations. After optimization, it was found that the energy of the left configuration is -721.249 Hartree, the energy of the middle configuration is -721.204 Hartree, the energy of the right configuration is -721.249 Hartree, the energies of the left and right configurations are the same, and the energy is lower. Hence, optimized left and right configurations are the stable configurations of DN-10. Due to the symmetric structure of N_2O_4, we set the symmetric initial configuration. After optimization, we find that the configuration is identical to the initial configuration, and the configuration energy is -409.994 Hartree, which is the stable structure of N_2O_4.

3.4.2. Reactivity

Kenichi Fukui [21] proposed the frontier orbital theory, which states that in a molecule, the electron in the highest occupied molecular orbital (HOMO) has the highest energy, is the least bound, and is the most likely to undergo a reduction reaction. In contrast, the lowest unoccupied molecular orbital (LUMO) has the lowest energy of all unoccupied orbitals, is the most likely to accept electrons, and is the most likely to undergo oxidation reactions. The difference in energy between HOMO and LUMO, ΔE (gap), reflects the activity of the molecule in reacting with free radicals [22]. The LUMO and HOMO energy level differences of DMAZ, DN-10, and N_2O_4 based on B3LYP/6-31+G (d, p) are calculated as shown in Table 3. As indicated, the energy level difference of DN-10 is larger than that of DMAZ, indicating that the reactivity of DN-10 is weaker than that of DMAZ, i.e., the stability of DN-10 is higher, and the conditions for the occurrence of the reaction are more demanding. This is consistent with the phenomenon that DN-10 and N_2O_4 ignition are difficult to initiate spontaneously at room temperature, but can be rapidly ignited and burned when heated.

Table 3. LUMO and HOMO of DMAZ, DN-10, and DMAZ/DN-10 formulated fuel

Molecular	LUMO, eV	HOMO, eV	MOs' Gap, eV
DN-10	-0.041	-0.250	0.209
DMAZ	-0.042	-0.203	0.161
N_2O_4	-0.151	-0.322	0.171

The formulated fuel with 10 % DN-10 must be heated to 35 ℃ to ignite and burn with N_2O_4, while DMAZ can ignite and burn with N_2O_4 at room temperature.

3.4.3. Active sites

3.4.3.1. Fukui function

The Fukui function is commonly used to predict reactive sites and is categorized into three types, which are used to predict nucleophilic, electrophilic, and free radical reactive regions, respectively. The reduced Fukui function quantifies the distribution of the Fukui function on each atom to predict the reaction sites of free radicals, and the reduced Fukui function f_0 of fuel is calculated by the difference of Hirshfeld's charge. The larger the value f_0 is, the more likely the free radical reaction will occur at that atom [23]. The structures of the DMAZ is shown in Fig. 7, the calculation results of the three substances are shown in Table 4 – Table 6.

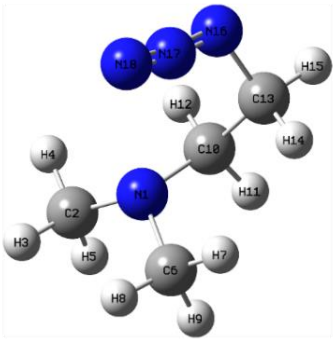


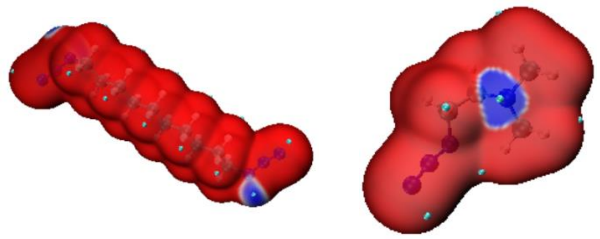
Fig. 7. Geometric configuration of DMAZ

As indicated, the Fukui function f_0 of 31(N) and 32(N) of DN-10 is the largest and most likely to be active sites; the Fukui function f_0 of 8(N) of DMAZ is the largest and most likely to be active sites; The Fukui functions f_0 of 3(O), 4(O), 5(O), and 6(O) of N_2O_4 are equal and maximum, and are most likely to be active sites, which provides a theoretical basis for the subsequent calculation of the hydrogen abstraction.

3.4.3.2. ALIE

The energy required to remove an electron from a point in the space of a molecular system is known as the ALIE, and the smaller the ALIE is, the weaker the electron is bound, the stronger the electronic activity is. The easier the free radicals react. Based on the generated wavefunction files, the red region of the ALIE electronic density isosurface is the region where the ALIE value of the molecule is larger [24]. Its electronic activity is weaker; the blue region of the ALIE electronic density isosurface is the

region where the ALIE value of the molecule is smaller, and its electronic activity is stronger. The cyan point of the ALIE electronic density isosurface is the point where the ALIE value of the molecule is minimal. As shown in Fig. 8, from the isosurface of ALIE ρ = 0.0005 a.u., it can be seen that the 3(N) of the DMAZ is the blue region, which is the most probable for the active sites.



a b

Fig. 8. a – ALIE isosurfaces of DN-10; b – ALIE isosurfaces of DMAZ

Combined with the analysis of the Fukui function, the most probable number for the active sites of the DMAZ is 3(N), which is different from the sites predicted by the Fukui function. Hence, the hydrogen abstraction of 3(N) and 8(N) sites of DMAZ and N_2O_4 will be calculated by considering both the Fukui function and ALIE results in the subsequent hydrogen abstraction calculation. 31(N) and 32(N) of DN-10 are blue areas, which means that the N of azide groups on both sides are most likely to be active sites, consistent with the Fukui function results. Comparing DMAZ and DN-10, the cyan area of DMAZ is larger, which indicates that the reactivity of DMAZ is larger. Determining the active sites and reactivity of the fuel provides the basis for the subsequent calculation of the hydrogen abstraction.

3.4.4. Hydrogen abstraction

The hydrogen abstraction paths of DMAZ and DN-10 with N_2O_4 were calculated at the B3LYP/6-31+G d) level of theory (see Fig. 9). Fig. 9 a – c show the hydrogen abstraction processes occurring at different positions of C atoms adjacent to 3(N) and C atoms adjacent to 8(N) for N_2O_4 and DMAZ, respectively. According to Fig. 9 a, the barrier of cis-HON_2O_3 was 18.92 kJ/mol, which is the lowest among the three DMAZ sites for hydrogen abstraction, indicating that this site is the most prone to H loss. Hence, the H on 1(C) adjacent to 3(N) was the most likely to be lost, resulting in hydrogen abstraction. Still, it was higher than that of hydrazine (hydrogen abstraction barrier = 3 – 15 kJ/mol), which is consistent with the longer ignition delay period of the DMAZ.

Table 4. Fukui function of DN-10

Atom	q(N)	q(N+1)	q(N-1)	f^-	f^+	f^0	CDD
17(C)	-0.045	-0.048	-0.036	0.008	0.003	0.006	-0.004
18(H)	0.025	0.022	0.031	0.006	0.003	0.004	-0.002
19(H)	0.025	0.022	0.031	0.006	0.003	0.005	-0.002
20(H)	0.027	0.023	0.032	0.006	0.003	0.004	-0.002
21(H)	0.027	0.022	0.033	0.006	0.004	0.005	-0.002
22(C)	-0.044	-0.049	-0.033	0.010	0.005	0.008	-0.004
23(C)	-0.053	-0.059	-0.037	0.014	0.006	0.010	-0.008
24(H)	0.027	0.021	0.035	0.008	0.006	0.007	-0.002
25(H)	0.028	0.021	0.037	0.009	0.007	0.008	-0.002
26(C)	0.006	-0.022	0.028	0.022	0.028	0.025	0.006
27(H)	0.032	0.022	0.043	0.011	0.010	0.010	-0.001
28(H)	0.026	0.022	0.034	0.008	0.004	0.006	-0.003
29(H)	0.034	0.010	0.058	0.024	0.024	0.024	-0.001
30(H)	0.048	0.025	0.068	0.020	0.023	0.022	0.002
31(N)	-0.122	-0.294	0.029	0.151	0.172	0.161	0.020
32(N)	-0.122	-0.294	0.029	0.151	0.172	0.161	0.020
33(N)	0.149	0.049	0.196	0.047	0.099	0.073	0.052
34(N)	-0.145	-0.237	-0.017	0.128	0.091	0.109	-0.036
35(N)	0.149	0.049	0.196	0.047	0.099	0.073	0.052
36(N)	-0.145	-0.237	-0.017	0.128	0.091	0.109	-0.036

Table 5. Fukui function of DMAZ

Atom	q(N)	q(N+1)	q(N-1)	f^-	f^+	f^0	CDD
1(C)	-0.046	-0.056	-0.001	0.045	0.010	0.027	-0.035
2(C)	-0.041	-0.053	0.004	0.046	0.012	0.029	-0.033
3(N)	-0.114	-0.112	0.116	0.230	-0.002	0.114	-0.233
4(C)	-0.001	-0.016	0.030	0.031	0.016	0.023	-0.015
5(C)	0.004	-0.052	0.024	0.019	0.056	0.038	0.036
6(N)	-0.128	-0.282	-0.101	0.026	0.154	0.090	0.127
7(N)	0.149	-0.044	0.180	0.030	0.193	0.112	0.163
8(N)	-0.119	-0.443	0.004	0.123	0.324	0.224	0.201
9(H)	0.032	0.008	0.073	0.040	0.024	0.032	-0.015
10(H)	0.033	0.020	0.073	0.040	0.012	0.026	-0.027
11(H)	0.023	0.002	0.081	0.058	0.020	0.039	-0.037

Table 6. Fukui function of N_2O_4

Atom	*q*(N)	*q*(N+1)	*q*(N-1)	*f*-	f_+	f_0	CDD
1(N)	0.241	0.125	0.325	0.083	0.116	0.099	0.033
2(N)	0.241	0.125	0.325	0.083	0.116	0.099	0.033
3(O)	-0.120	-0.312	0.087	0.208	0.191	0.200	-0.016
4(O)	-0.120	-0.312	0.087	0.208	0.191	0.200	-0.016
5(O)	-0.120	-0.312	0.087	0.208	0.191	0.200	-0.016
6(O)	-0.120	-0.312	0.087	0.208	0.191	0.200	-0.016

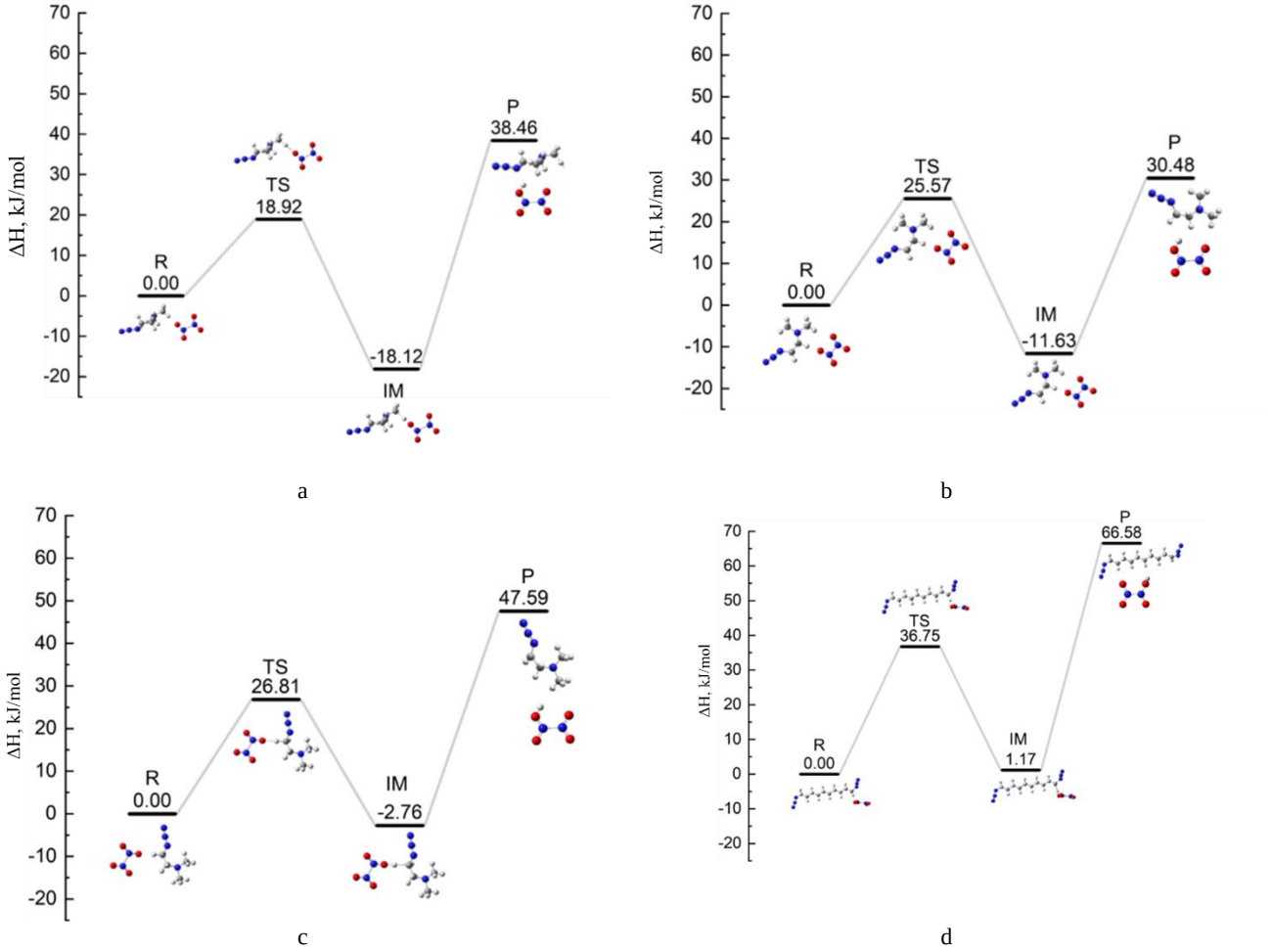


Fig. 9. a – hydrogen extraction reaction between N_2O_4 and 1 (C) atom adjacent to 3 (N) in DMAZ; b – hydrogen extraction reaction between N_2O_4 and 4 (C) atom adjacent to 3 (N) in DMAZ; c – hydrogen abstraction of DMAZ and N_2O_4 with 8(N) as active sites; d – hydrogen abstraction of DN-10 and N_2O_4

The longer ignition delay of DMAZ may be due the lower reactivity of the azide group compared to the amine N atoms, resulting in its hydrogen abstraction barrier being higher than that of hydrazine. Based on their hydrogen abstraction barriers, the 3(N) position of DMAZ is most likely to be the reaction active site, which is consistent with ALIE calculations. Fig. 9 d shows the hydrogen abstraction on the C adjacent to 31(N) in DN-10, and the barrier for the generation of cis-HON_2O_3 from DN-10 was 36.75 kJ/mol, exceeding the hydrogen abstraction barriers of DMAZ. The higher the barrier, the more difficult it is to break the bond in the reaction, and the more difficult the reaction becomes. This also explains why the formulated fuel, after adding DMAZ in the experiment, is difficult to ignite at room temperature but can be ignited after heating. Meanwhile, when comparing the enthalpy change of hydrogen abstraction, DN-10 was 66.58 kJ/mol, much larger than that of DMAZ. This also indicates that more energy needs to be absorbed during the reaction, and the reaction is barely possible at low temperatures, which is consistent with the experimental results.

4. CONCLUSIONS

The key properties of DMAZ/DN-10 formulated fuel and N_2O_4 were investigated by combining theoretical calculations and experimental validation. Based on the experimental results, DFT-based theoretical calculations of the DMAZ, DN-10, and N_2O_4 reaction kinetics were carried out. The following conclusions were drawn:

1. DMAZ/DN-10 formulated fuel density increased significantly, and the viscosity below 30% of DN-10

was well maintained, meeting the requirements of high density and low-temperature fluidity.

2. The combustion heat of formulated fuel was significantly higher than that of DMAZ, and the net combustion heat of formulated fuel with 70% DN-10 increased by 12.1 %, but since the ignition of formulated fuel occurred only at elevated temperatures, it required heating.
3. The experimental results and DFT-based calculations of ignition delay revealed that the reactivity of DN-10 was lower than that of DMAZ, and hydrogen abstraction barrier for DN-10 to generate cis-HON_2O_3 was larger than that of DMAZ, the more difficult to occur the reaction; the greater the enthalpy change of hydrogen abstraction, the more heat needs to be absorbed in the reaction process. This explains the experimental phenomenon and provides a theoretical basis for the next step of formulated fuel optimization.

Acknowledgements

This work was supported by the Shaanxi Provincial Natural Science Foundation (Grant No. 2023-JC-YB-138).

REFERENCES

1. **Wu, Y., Kong, X., Ao, Y., Hou, X., Wang, J., Yin, G., Sun, W., Zhang, Z., Tang, C.** Experimental and Kinetic Modeling Study on the Low-temperature Decomposition and Autoignition of 2-Azido-N,N-dimethylethanamine: A Promising Green Mono- and Bi-propellant *Proceedings of the Combustion Institute* 40 2024: pp. 1 – 7. https://doi.org/10.1016/j.proci.2024.105359
2. **Pradhan, S.K., Kedia, V., Kour, P.** Review on Different Materials and Their Characterization as Rocket Propellant *Materials Today: Proceedings* 33 (8) 2020: pp. 5269 – 5272. https://doi.org/10.1016/j.matpr.2020.02.960
3. **Iranizadeh Hamid, R., Ghanbari, P., Shahram, Bahri, R., Mohammad, M.** Effect of Oxidizer to Fuel Ratio on Tank Mass and Thickness for Liquid Fuel Dimethyl Aminoethyl Azide (DMAZ) with Some Oxidizers in Space Programs *Iranian Journal of Chemistry & Chemical Engineering-international English Editio* 42 (10) 2023: pp. 3480 – 3486.
4. **Meng, X., Jia, Y., Xu, L., Li, J.** Hydrazine Based Fuel Color Changing Active Materials and Carrier Compatibility Testing C*hemical Propellants and Polymer Materials* 22 (6) 2024: pp. 67 – 72.
5. **Jin, G., Huang, Z., Huang, Y., Gao, M., Wang, Y.** Kinetic Simulation of the Reaction Between N,N dimethylazidoethylamine (DMAZ) and Dinitrogen Tetroxide (NTO) based on Density Functional Theory *Structural Chemistry* 36 (10) 2025: pp. 807 – 815. https://doi.org/10.1007/s11224-024-02401-6
6. **Joshua, M., Morgan, L., Dimitris, K., Lucas, M., Jeffrey, D, Risha, G.A.** Combustion of a TMEDA/WFNA Hypergolic in a Bipropellant Rocket Engine *AIAA Propulsion and Energy Forum* 2019: pp. 1 – 8. https://doi.org/10.2514/6.2019-4155
7. **Pakdehi, S., Taffazolinia, H., Rezaei, S., Fathollahi, M.** Effect of Some Chemical Additives in Increasing the Electrical Conductivity of the Liquid Fuel Dimethyl Aminoethyl Azide (DMAZ) *Central European Journal of Energetic Materials* 19 (3) 2022: pp. 264 – 280. https://doi.org/10.22211/cejem/154826
8. **Rouhandeh, H., Shahram, G., Bahri, M.M., Valizadeh, E.** Performance Assessment of Binary Liquid Fuels DMAZ-TMEDA with Some Nitric Acid-Based Oxidizers *Arabian Journal for Science and Engineering* 48 2023: pp. 8359 – 8369. https://doi.org/10.1007/s13369-022-06910-6
9. **Wang, S., Thynell, S., Chowdhury, A.** Experimental Study on Hypergolic Interaction Between N, N, N', N'-tetramethylethylenediamine and Nitric Acid *Energy & Fuels* 24 (10) 2010: pp. 5320 – 5330. https://doi.org/ 10.1021/ef100593s
10. **Liu, W., Dasgupta, S., Zybin, S., Goddard, W.** First Principles Study of Theignition Mechanism for Hypergolic Bipropellants: N, N, N',N'-tetramethylethylenediamine (TMEDA) and N, N, N',N'-tetramethylmethylenediamine (TMMDA) with Nitric Acid *Journal of Physical Chemistry A* 115 (20) 2011: pp. 5221 – 5229. https://doi.org/10.1021/jp202021s
11. **Zhao, J., Huang, Z., Jin, G., Zhu, H.** Research Progress on Ignition Delay Mechanism and Determination of Azide Amine *Chemical Propellants and Polymer Materials* 19 (3) 2021: pp. 8 – 13.
12. **Kang, H., Park, S., Park, Y., Lee, J.** Ignition-delay Measurement for Drop Test with Hypergolic Propellants: Reactive Fuels and Hydrogen Peroxide *Combustion and Flame* 217 2020: pp. 306 – 313. https://doi.org/10.1016/j.combustflame.2020.04.017
13. **Liao, X., Lu, R., Xia, L., Liu, Q., Wang, H., Zhao, K., Wang, Z., Zhao, Y.** Density Functional Theory for Electrocatalysis *Energy and Environmental Material* 1 (5) 2022: pp. 157 – 185. https://doi.org/10.1002/eem2.12204
14. **Axel, D.** Perspective: Fifty Years of Density-functional Theory in Chemical Physics *Energy and Environmental Material* 140 (18) 2014: pp. 18A301-1 – 18A301-18. https://doi.org/10.1063/1.4869598
15. **Shahram, G.P, Bahman, S.** The Effec tof Some Amines on Ignition Delay Time of Dimethyl Amino Ethyl Azide(DMAZ) and White Fuming Nitric Acid(WFNA) *Propellants Explosives Pyrotechnics* 42 2017: pp. 1 – 9. https://doi.org/10.1002/prep.201700208
16. **Zhang, P., Zhang, L., Chung, K.** Density Functional Theory Study of the Reactions of 2-azido-N,N-dimethylethanamine with Nitric Acid and Nitrogen Dioxide *Combustion and Flame* 162 2015: pp. 237 – 248. https://doi.org/10.1016/j.combustflame.2014.06.016
17. **Lemi, T.** Interaction of DMAZ and TEMED – A DFT Treatise *Earthline Journal of Chemical Sciences* 9 (2) 2023: pp. 163 – 176. https://doi.org/10.34198/ejcs.9223.163176
18. **Chen, C., Michael, J.** Mechanisms and Kinetics for the Thermal Decomposition of 2-azido-N,N-dimethylethanamine (DMAZ) *The Journal of Physical Chemistry A* 14 (116) 2012: pp. 3561 – 3576. https://doi.org/10.1021/jp212079f
19. **Wang, H., Sun, X., Zhou, Y., Liu, G., Wang, Y., Cao, J.** Study on the Thermal Decomposition Mechanism and Reaction Dynamics of Spiral [4,5] - Decane and Spiral [5,6] - Dodecane Fuels *Journal of Fuel Chemistry* 52 (7) 2024: pp. 1021 – 1034.
20. **Markus, B., Jan-Michael, M., Andreas, H., Stefan, G.** Best-Practice DFT Protocols for Basic Molecular Computational Chemistry *Angewandte Chemie* 134 (42) 2022: pp. 1 – 27. https://doi.org/10.1002/ange.202205735

21. **Maylis, O., Dimitrios, A., Frank, N.** Density Functional Theory *Photosynthesis Research* 102 2009: pp. 443 – 453. https://doi.org/10.1007/s11120-009-9404-8
22. **Zhao, J., Huang, Z., Jin, G., Gao, M., Zhu, H.** Reaction Kinetics Simulation of Hydrazine Fuel and NO_2 Gas-phase Hydrogen Extraction *Energetic Materials* 29 (11) 2021: pp. 1125 – 1131.
23. **Cao, J., Ren, Q., Chen, F.** Comparative Study on the Methods for Predicting the Reactive Site of Nucleophilic Reaction *Science China Chemistry* 58 2015: pp. 1845 – 1852. https://doi.org/10.1007/s11426-015-5494-7
24. **Chen, E., Tang, L.** 1981 Nobel Prize in Chemistry Winner Kenichi Fukui and His Theory *Chemistry* 5 1982: pp. 36 – 42.

© Gao et al. *2026* Open Access This article is distributed under the terms of the Creative Commons Attribution 4.0 International License (http://creativecommons.org/licenses/by/4.0/), which permits unrestricted use, distribution, and reproduction in any medium, provided you give appropriate credit to the original author(s) and the source, provide a link to the Creative Commons license, and indicate if changes were made.